# Challenges in Orbital Debris Modeling: A Comparative Analysis of NASA SBM and Space Fence Data

**Tory Smith,**[*] **Zachary Folcik,**[†] **Richard Linares**[‡]
*Massachusetts Institute of Technology*
*MIT Lincoln Laboratory*

## ABSTRACT

This paper presents case studies of the A/M distributions and $\Delta V$ distributions estimated by the NASA Standard Break-up Model (SBM) when compared against empirical data. We use data collected by the Space Fence phased array radar and gathered by MIT Lincoln Laboratory (MIT/LL) for five recent break-up events before modeling the same events with the NASA SBM and comparing the resulting distributions. NASA developed their model for satellite break-ups in the 1990s with hypervelocity ground tests and radar observation data of on-orbit break-ups. The model has since become the go-to for orbital capacity and long-term population evolutionary models such as NASA's own LEGEND, and the MIT Orbital Capacity and Analysis Tool (MOCAT). Its ease of implementation and low computational cost makes it an attractive option for modeling fragmentation events within these environment models. Now that the Space Fence has been operational for several years and has observed several on-orbit break-up events, opportunities have emerged to further investigate and characterize any discrepancies that may exist between the current NASA break-up model and new empirical data. The SBM is broken into three parts: size distributions, A/M distributions, and $\Delta V$ distributions. In a previous study, we compared the size distributions estimated by the NASA SBM when modeling these events against the empirical data from the debris cloud of the same events captured by Space Fence. In this paper, we will continue our investigation of the NASA SBM by comparing the results of the SBM's A/M distributions and $\Delta V$ distributions against the data collected by Space Fence for the same events studied previously.

## 1. INTRODUCTION

As the space environment becomes more congested [26], it is imperative that we have a proper understanding of the effects of that congestion as we look to maintain humanity's continued use of space. One of our best tools for this purpose are population evolutionary models which seek to estimate the near-Earth environment in the near-term to long-term [10, 11, 14, 20]. These tools allow policy makers, space operators, commercial companies, and other stakeholders to be informed when making decisions on the capacity of the space environment, effects of launch rate, or the impacts of one or several missions.

One of the most crucial components if these models is the estimation of debris caused by satellite fragmentation events in terms of size, area-to-mass (A/M) ratio, and $\Delta V$ distributions, either from an explosion, or a collision. Modeling these events presents significant challenges due to the numerous variables involved, such as the impact geometry, relative velocity, mass of the objects and the complex material interactions, during hypervelocity impacts for collision scenarios, which rapidly escalate computational complexity [12, 32]. To address these challenges, three primary approaches are typically used in developing break-up models: numerical, empirical, and semi-empirical [12,15,23,32]. Numerical models employ hydrocodes [22, 32] that simulate the deformation process and evolving geometry during the break-up event by incrementally applying conservation equations along with constitutive equations for material behavior [32, 35, 37]. These models offer the highest fidelity and most accurately replicate real-world break-up events [32]. However, they are computationally intensive and require extensive information about the event, such as 3D satellite mock-ups and impact geometry [32]. Empirical models, on the other hand, use statistical methods to derive functions that align with data from experiments and on-orbit observations [15]. These models are easy to implement

---

[*]PhD Student, Department of Aeronautics and Astronautics, E-mail: tsmith2@mit.edu
[†]Technical Staff, MIT Lincoln Laboratory, E-mail: folcik@ll.mit.edu
[‡]Associate Professor, Department of Aeronautics and Astronautics. E-mail: linaresr@mit.edu

and can accurately represent events within the data range used for model development [15]. However, they often lack inherent conservation of physical properties, such as mass, and need non-physics-based supplemental functions to correct initial estimates [19]. Their accuracy diminishes when modeling break-ups outside the collected data range, such as those involving modern satellite materials [24], and they do not account for factors like impact location [15]. Semi-empirical models aim to balance the computational simplicity of empirical models with the higher fidelity of numerical models. They use conservation laws to constrain empirical results, enabling internally consistent predictions without the high computational demands of hydrocodes [12]. These models can incorporate factors like satellite structure and impact location and range from simpler, empirically-based and computationally efficient models [23] to more detailed and computationally intensive ones [12].

As population evolutionary models often require thousands of Monte Carlo trials to produce a proper range of estimates, computational efficiency becomes extremely important [14]. This leads developers of these models to lean more heavily on empirical and semi-empirical break-up models, of which, the NASA Standard Break-up Model (SBM) has become the most commonly employed. However, in recent years, deficiencies in the NASA SBM have been identified when compared against ground-based tests such as the DebriSat experiment [24] and numerical simulations [32]. To compliment this work, we wished to investigate the accuracy of the NASA SBM against observations of recent on-orbit break-ups. To do so, we collected observations made by Space Fence of five recent break-ups: COSMOS 1408 anti-satellite (ASAT) test, Chang Zheng 6A, H-IIA Launch Vehicle, COSMOS 2499, and Orbcomm FM36. In a previous paper, we investigated the accuracy of the size distributions estimated by the SBM against these observations. In this paper, we continue our investigation by examining the A/M and $\Delta V$ distributions generated by the SBM against that same data. We first aggregate the observations made by Space Fence, including RCS, range, and range-rate, convert the radar measurements into A/M and $\Delta V$ distributions and then compare this data to distributions estimated by the SBM for the same events.

## 2. BREAK-UP EVENTS

As break-up events are rare, there are few examples of events captured by Space Fence for our comparison making it difficult to sample a wide variety of events for comparison to the SBM. Under this data limitation, we gathered observations from the five following break-up events for our study:

- COSMOS 1408 ASAT Test: On 15 November 2021, Russia conducted a destructive test with a direct-ascent ASAT missile against one of its own satellites, COSMOS 1408. Original estimates for the number of debris pieces caused by the collision vary depending on the source but are roughly on the order of magnitude of 1500 pieces [21] [28]. During the first pass through Space Fence, we were able to establish tracks for 1665 objects.

- Chang Zheng 6A: On 12 November 2022, an upper-stage rocket body from a Chinese launch vehicle broke apart in orbit. In a Twitter post on 13 November, the USSF 18th Space Defense Squadron (SDS) announced that they were tracking over 50 pieces of debris from the rocket explosion [16]. In a later update, the number of debris from the event was estimated as 350 pieces [30]. We identified 238 objects observed by Space Fence in the first 12-hour period after the event.

- H-IIA Launch Vehicle: On 3 July 2022, the 18th SDS confirmed the break-up of a Japanese rocket fairing from the H-IIA launch vehicle, most likely caused by a collision from a lethal non-trackable object [25]. We were able to establish tracks for 69 objects associated with the event.

- COSMOS 2499: On 3 January 2023, a Russian satellite known as COSMOS 2499 fragmented into 150 objects observable by Space Fence. The cause of the event is believed to be an explosion [3]

- Orbcomm FM36: On 11 March 2023, a US communications satellite from the Orbcomm constellation fragmented due to an explosion [3] of which we were able to form tracks for 55 objects correlated with the event.

## 3. METHODOLOGY

### 3.1 Space Fence Data Collection

The United States Space Force (USSF) uses a multitude of sources for gathering observations related to objects orbiting the earth to ensure the safety and security of military, civil, and commercial space assets. One of the newest and most

robust of these assets is the Space Fence S-band phased array radar, capable of detecting objects as small as 1-2cm in length in low-earth orbit (LEO) [6].

To compare the NASA SBM predictions with the truth data collected by Space Fence, it is essential to first identify which pieces of orbital debris are associated with each break-up event or collision. Since debris can de-orbit shortly after the fragmentation event, only tracks observed during the first few passes through Space Fence's field of view following the event epoch are included in the analysis.

Space Fence observations are routinely processed using a MIT/LL system called Osiris. This prototype system facilitates residual plotting against known trajectories for all Space Fence observations. Notably, the prototype allows for the plotting of observations that have not been correlated with any known resident space object (RSO), referred to as uncorrelated tracks (UCTs). For each break-up event in this study, the trajectory of the original satellite was loaded for the period immediately preceding the event. Subsequently, all uncorrelated Space Fence observations were loaded into the Osiris display for the following 12-hour period. By displaying the residuals of these UCT observations against the known RSO trajectory—specifically examining the Beta angle, time, and height [7]—trends in the UCT plots became apparent, indicating their association with the original satellite trajectories. Using this technique, many UCT residuals showed linear slopes radiating outward from the event time and location. These slopes, along with the similarities in the UCT orbital plane to the original satellite trajectories, enabled the use of the Osiris display to identify and label these UCTs as belonging to the break-up events. Once all UCTs were labeled, the data was exported for our analysis here.

When estimating the sizes, or characteristic length ($L_c$) of the fragments for use in the Area-to-mass ratio calculations, we used the NASA Size Estimation Model [38]. As described in a previous paper [34], we summed each of the dipolar RCS measurements in dB before feeding them into the SEM [13]. We then took the average over the $L_c$s estimated by the SEM of each object array and used this as our $L_c$ for the object. It should be noted that because we are using the first 12-hour period, we are only obtaining between five and fifteen measurements for each object. This leads to the possibility of over fitting our estimations to these few observations. In future work, we hope to include more observations to improve the robustness of our investigation.

### 3.2 Deriving $\Delta V$ from Space Fence Observations

To find the velocities of objects observed by Space Fence, we used the methods as described by Vallado et al [1] for converting azimuth, elevation, range, and range-rate into the Earth Centered Inertial (ECI) frame. To verify our implementation, we converted the most recent Two-Line Element (TLE) provided by Space-Track.org [5] of the objects before their break-ups and propagated them in time to the last observation of the object by Space Fence using SGP4 [1]. When comparing the most recent TLE from the COSMOS 1408 ASAT to our converted observation, we found a difference in velocity of less than 10cm/s.

Using this method, we could find the $\Delta V$ of the objects resulting from a break-up by taking the difference between the velocity of the propagated TLE to the time of observation of the fragments and the velocity of the fragments observed by Space Fence after the break-up. To account for the effects of atmospheric drag, we used the estimated A/M of the fragments to find the modified ballistic coefficient (B*) used in SGP4 of the fragments using Eq. 1 and a flat plate drag coefficient ($C_d$) of 2.2 [36]. As Space Fence provides multiple observations of an object during a single pass, we took the average velocity over these observations as our value when evaluating the difference from the propagated TLE, as will be shown in Section 4.

$$B^* = \frac{1}{2}\frac{C_D A}{m}\rho_0 R_\oplus \tag{1}$$

where $\rho_0$ is the atmospheric density at perigee, assumed to be $\rho_0 = \frac{2.461 \times 10^{-5}}{ER} kg/m^2/ER$ with $ER = 6375.135$ km, and $R_\oplus = 6378.135$ km [36].

### 3.3 NASA Satellite Standard Break-up Model

Originally developed in 2001 for use in NASA's EVOLVE 4.0 orbital debris model [15] the SBM is based on a set of empirical relationships derived from ground-based laboratory experiments and observations of in-space fragmentation events.

The SBM is broken into three parts: Size Distributions, A/M Distributions, and $\Delta V$ Distributions. Each of these parts relies on at least one of the others to form a complete picture of a break-up. Each part of the model is then further

divided depending on whether an event is modeled as an explosion or a collision. In a previous paper [34], we provide a detailed description of the size distributions and A/M distributions. In this paper, we will briefly reiterate the A/M piece as necessary for context as well as describe the $\Delta V$ distribution calculation in full.

### 3.3.1 Area-to-Mass Ratio

The A/M distribution of a break-up uses a set of Normal distributions ($N$) with a weighting function ($\alpha$), mean ($\mu$) and standard deviation ($\sigma$) reliant on empirically derived relationships with the characteristic lengths ($L_c$) of thousands of objects cataloged in the SSN [15]. As described in [33] and [17], $L_c$ of objects resulting from a break-up are determined by the type of event (explosion, or collision), by the masses of the objects involved and the relative velocity in the case a collision. For objects with a characteristic length greater than 11cm, Johnson et al. [15], describes the following distribution:

$$D_{A/M} = \alpha(\lambda_c) \cdot N(\mu_1(\lambda_c), \sigma_1(\lambda_c), X) + (1 - \alpha(\lambda_c)) \cdot N(\mu_2(\lambda_c), \sigma_2(\lambda_c), X)$$
$$\text{where } \lambda_c = log_{10}(L_c) \tag{2}$$
$$X = log_{10}(A/M)$$

In this range, the parameters of the distribution are determined by the parent object type (rocket body (R/B), or spacecraft fragment (S/C)). The parameters for the R/B case are found with the following piecewise functions:

$$
\begin{aligned}
\alpha^{R/B} &= \begin{cases} 1 & \lambda_c \leq -1.4 \\ 1 - 0.3571(\lambda_c + 1.4) & -1.4 \leq \lambda_c < 0 \\ 0.5 & \lambda_c \geq 0 \end{cases} \\[2mm]
\mu_1^{R/B} &= \begin{cases} -0.45 & \lambda_c \leq -0.5 \\ -0.45 - 0.9(\lambda_c + 0.5) & -0.5 \leq \lambda_c < 0 \\ -0.9 & \lambda_c \geq 0 \end{cases} \\[2mm]
\sigma_1^{R/B} &= 0.55 \\[1mm]
\mu_2^{R/B} &= -0.9 \\[1mm]
\sigma_2^{R/B} &= \begin{cases} 0.28 & \lambda_c \leq -1.0 \\ 0.28 - 0.1636(\lambda_c + 1) & -1.0 \leq \lambda_c < 0.1 \\ 0.1 & \lambda_c \geq 0.1 \end{cases}
\end{aligned}
\tag{3}
$$

With corresponding piecewise functions for the S/C case:

$$\alpha^{S/C} = \begin{cases} 0 & \lambda_c \leq -1.95 \\ 0.3 - 0.4(\lambda_c + 1.2) & -1.95 \leq \lambda_c < 0.55 \\ 1 & \lambda_c \geq 0.55 \end{cases}$$

$$\mu_1^{S/C} = \begin{cases} -0.6 & \lambda_c \leq -1.1 \\ -0.6 - 0.318(\lambda_c + 1.1) & -1.1 \leq \lambda_c < 0 \\ -0.95 & \lambda_c \geq 0 \end{cases}$$

$$\sigma_1^{S/C} = \begin{cases} 0.1 & \lambda_c \leq -1.3 \\ 0.1 + 0.2(\lambda_c + 1.3) & -1.3 \leq \lambda_c < -0.3 \\ 0.3 & \lambda_c \geq -0.7 \end{cases} \tag{4}$$

$$\mu_2^{S/C} = \begin{cases} -1.2 & \lambda_c \leq -0.7 \\ -1.2 + 1.333(\lambda_c + 0.7) & -0.7 \leq \lambda_c < -0.1 \\ -2.0 & \lambda_c \geq -0.1 \end{cases}$$

$$\sigma_2^{S/C} = \begin{cases} 0.5 & \lambda_c \leq -0.5 \\ 0.5 - (\lambda_c + 0.5) & -0.5 \leq \lambda_c < -0.3 \\ 0.1 & \lambda_c \geq -0.3 \end{cases}$$

For fragments with $L_c$ smaller than 8cm the A/M distribution was derived from the SOCIT experiments [15]:

$$D_{A/M}^{SOC} = N(\mu_{SOC}(\lambda_c), \sigma_{SOC}(\lambda_c), X) \tag{5}$$

Unlike fragments above 11cm, the parameters for these equations are not reliant on the type of parent object:

$$\mu^{SOC} = \begin{cases} -0.3 & \lambda_c \leq -1.75 \\ -0.3 - 1.4(\lambda_c + 1.75) & -1.75 \leq \lambda_c < -1.25 \\ -1.0 & \lambda_c \geq -1.25 \end{cases}$$

$$\sigma^{SOC} = \begin{cases} 0.2 & \lambda_c \leq -3.5 \\ 0.2 + 0.1333(\lambda_c + 3.5) & \lambda_c > -3.5 \end{cases} \tag{6}$$

Finally, for fragments between 8cm and 11cm, a bridging function is employed that uses a combination of the previous distributions.

$$D_{A/M}^{Bridge} = \beta \cdot D_{A/M}(\lambda_c, X) + (1 - \beta) \cdot D_{A/M}^{SOC}(\lambda_c, X)$$
$$\text{where } \beta = \frac{L_c - 0.08}{0.03} \tag{7}$$

When estimating the A/M for objects observed by Space Fence, we use these same functions described above for converting the $L_c$ of the observed objects for comparison to the estimated values by the SBM.

### 3.3.2 $\Delta V$ Distribution

When calculating the $\Delta V$ of the objects resulting from a fragmentation event, the SBM uses A/M as the independent variable for Normal distributions with empirically derived parameters in a similar fashion to the A/M distributions. Using A/M as the independent variable, NASA discovered similar distributions formed for explosions and collisions [15] with only slightly different parameters.

For an explosion, the following distribution and parameters are employed:

$$D_{\Delta V}^{EXP}(X,v) = N(\mu^{EXP}(X), \sigma^{EXP}(X), v)$$
$$\text{where } X = log_{10}(A/M)$$
$$v = log_{10}(\Delta V) \tag{8}$$
$$\mu^{EXP} = 0.2X + 1.85$$
$$\sigma^{EXP} = 0.4$$

With the corresponding distribution employed for collisions:

$$D_{\Delta V}^{COLL}(X,v) = N(\mu^{COLL}(X), \sigma^{COLL}(X), v)$$
$$\text{where } \mu^{COLL} = 0.9X + 2.9 \tag{9}$$
$$\sigma^{EXP} = 0.4$$

## 4. RESULTS

In this section, we compare the results of the A/M distributions and $\Delta V$ distributions produced by the NASA SBM against the observations made by Space fence for the five break-up events described in 2. For the S-band Space Fence radar, detection of small objects ($< 10cm$) is less probable so tracks can't be formed for every object detected. For our investigation, we set the lower-bound of comparison to 10cm to avoid extrapolation of the data to compensate for the probability of detection. Notably, this means we are unable to compare the portion of the A/M distributions exclusively below 8cm from Equation 6 and are only able to compare against Equation 2 for objects above 11cm and from the bridging function in Equation 7 above 10cm, which will have maximum weighting from the below 8cm distribution, as set by $\beta$, of 0.33.

### 4.1 COSMOS 1408 ASAT Test

We discussed this event in detail in our previous paper, and the controversies about its nature [34]. The mass of the primary object (COSMOS 1408) is estimated to be 1750 kg [21], and the mass of the secondary object (the Russian ASAT) is estimated to be 63.5 kg. We used the Raytheon missile interceptor kill-vehicle as a corollary due to lack of publicly available information about the actual projectile [31]. The relative velocity between the two objects, 4.6 km/s, was determined based on information published by COMSPOC Corporation [27]. Parameters used in the SBM are summarized in Table 1.

Table 1: NASA SBM Input Parameters: COSMOS 1408 ASAT Test

| Model Inputs | Value | Units |
|---|---|---|
| Primary Object Mass | 1750 | kg |
| Primary Object Radius | 2.5 | m |
| Secondary Object Mass | 63.5 | kg |
| Relative Velocity | 4.6 | km/s |

#### 4.1.1 A/M Distribution

As mentioned previously, the data gathered by Space Fence is inconsistently detectable as the debris sizes reduce to the limits of the S-band. For a proper comparison, we limit our comparison to sizes larger than 10 cm and below 1m as that is the upper limit for the power law used by the SBM. The results of the comparison between the SBM and Space Fence can be seen in Fig. 1.

Figures 1a and 1b show a strong correlation between the SBM and the data collected by Space Fence for this event. The only discernible difference is a slightly tighter concentration of objects around an A/M of 0.1 $\frac{m^2}{kg}$ for Space Fence as compared to the SBM. However, as the SBM is a general model, a slight variation between scenarios is expected and we considered this event captured well by the SBM for objects within the range of evaluation.

(a) A/M Vs. Characteristic Length        (b) $log_{10}(A/M)$ Distribution
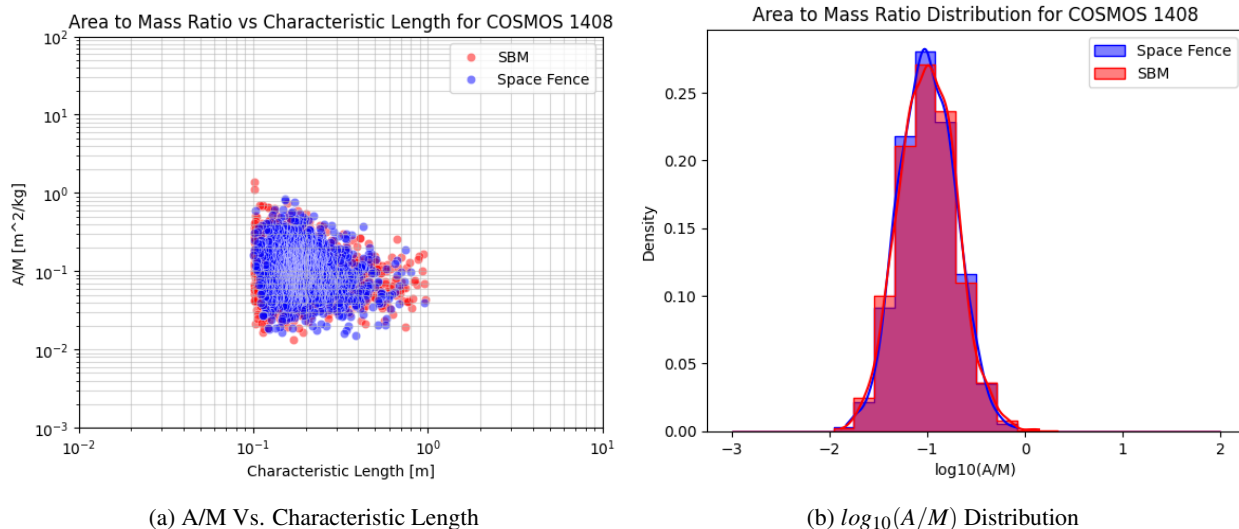
Fig. 1: A/M distribution comparison between Space Fence data and the NASA SBM for the 1408 ASAT test

### 4.1.2 $\Delta V$ Distribution

As the $\Delta V$ distribution uses the A/M as the independent variable, this inherently limits our comparison to objects within the threshold used for the A/M comparisons. The results of the $\Delta V$ distribution comparison can be seen in Fig. 2
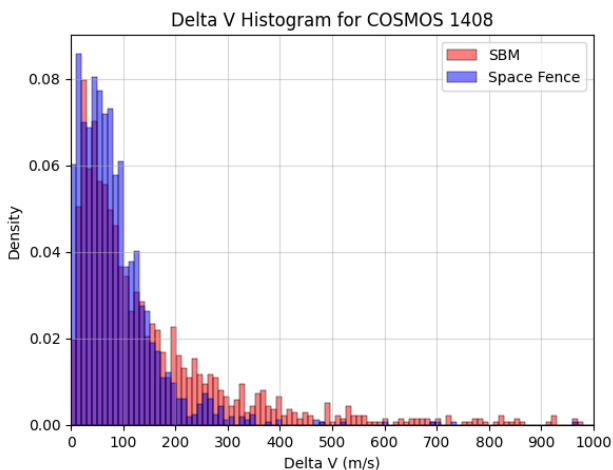


Fig. 2: $\Delta V$ distribution comparison between Space Fence data and the NASA SBM for the COSMOS 1408 ASAT test

Unlike the A/M distribution, we see less correlation between the SBM and the data collected by Space Fence. As shown in Fig. 2 the objects generated by the ASAT are concentrated at lower $\Delta V$s than what is estimated by the SBM. Using a bootstrapped p-value through a Cramér-von Mises (CvM) criterion [8] as quantitative measure of the discrepancy between the two distributions, we find a p-value near 0, suggesting a statistically significant difference between the two distributions. As there are some unknowns about the projectile used in this event, such as the mass and exact relative velocity, it's possible that with the limited information we have available that we are not modeling the event correctly and additional factors may cause the discrepancies. However, with the information and estimations we do have, the SBM does not seem able to capture this event accurately in terms of $\Delta V$.

## 4.2 Chang Zheng 6A

This event can be attributed to an explosion according to the March 2023 NASA Orbital Debris Quarterly [4]. Since the Chinese rocket specifications are not publicly available, we based our mass and radius estimations on the US equivalent rocket specifications [9]. The parameters of our NASA SBM analysis for the Chang Zheng 6A fragmentation event is shown in Table 2.

Table 2: NASA SBM Parameters: Chang Zheng 6A

| Model Inputs | Value | Units |
|---|---|---|
| Primary Object Mass | 952 | kg |
| Primary Object Radius | 3.0 | m |

### 4.2.1 A/M Distribution

Similar to the comparisons made between the SBM and the Space Fence data for COSMOS 1408, we limit our margins of comparison to object above 10cm and below 1m. The results can be seen in 3



(a) A/M Vs. Characteristic Length

(b) $log_{10}(A/M)$ Distribution
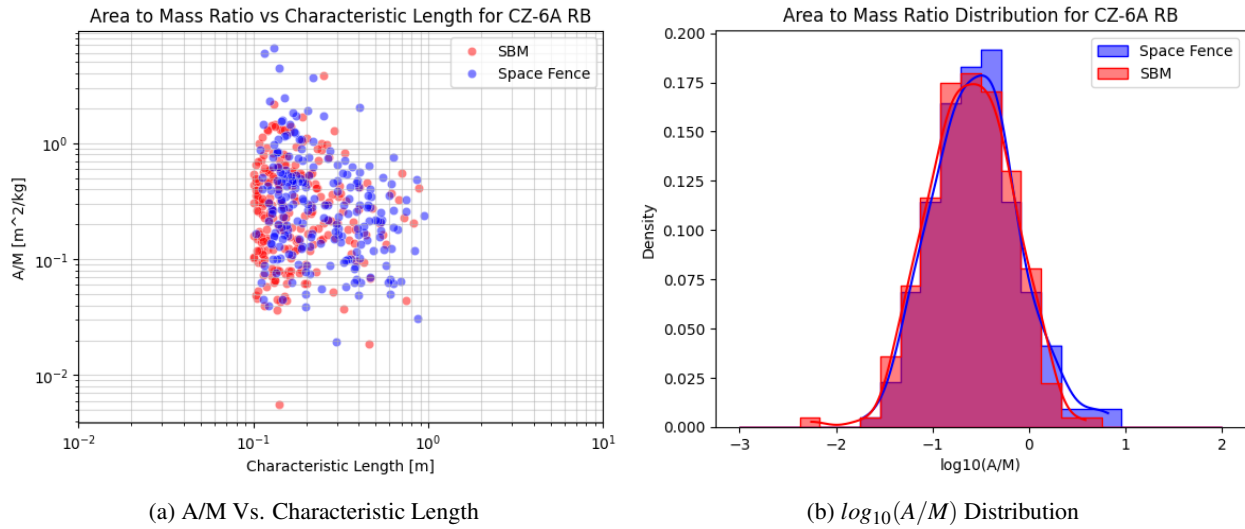
Fig. 3: A/M distribution comparison between Space Fence data and the NASA SBM for the CZ6A Explosion

This event also matches well between the observed data and that estimated by the SBM with a near perfect distribution match for the $log(A/M)$ as shown in figure 3b. The slightly tighter distribution of the Space Fence data, this time around an A/M of 0.05 $\frac{m^2}{kg}$, can be attributed to the stochastic nature of the A/M distribution estimations of both Space Fence and the SBM.

### 4.2.2 $\Delta V$ Distribution

As with the COSMOS 1408 break-up the $\Delta V$ distribution is limited to the aforementioned 10cm to 1m margins due to the inconsistency of detection below 10cm and objects no longer following the power law in the SBM above 1m. The results of the comparison for the CZ6A explosion event can be seen in Fig. 4
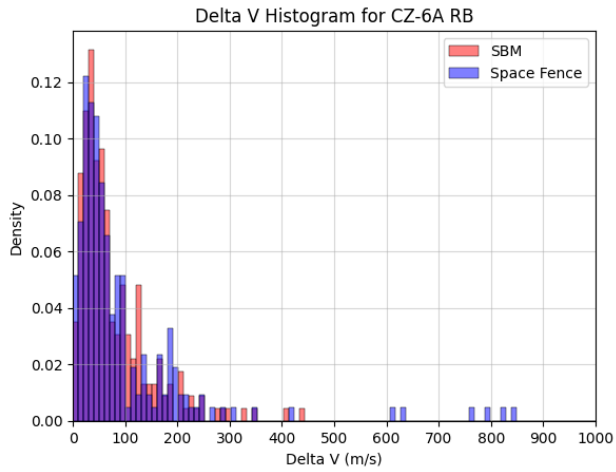
Fig. 4: $\Delta V$ distribution comparison between Space Fence data and the NASA SBM for the CZ6A Explosion

Unlike the COSMOS 1408 results shown in Fig. 2, we see a strong agreement between the $\Delta V$ distribution estimated by the SBM when compared against the observations collected by Space Fence. Notably, the slight discernible difference between the SBM and empirical data is an overestimation of lower $\Delta V$ objects by the SBM, which is in contrast to what we saw for COSMOS 1408. However, using the same bootstrap p-value CvM technique as described earlier, we find a p-value of 0.8418 which suggests there is very little difference between the two distributions.

### 4.3 H-IIA Launch Vehicle

NASA attributed this event to a collision with a lethal non-trackable (LNT) [3] due to its lack of energy storage devices. This makes the event particularly difficult to model as we must estimate the mass, size and relative velocity of the secondary object involved in the event with no information other than that it was small enough to not be trackable by current SDA capabilities. With these limitations, we decided to estimate the secondary object as an aluminum or stainless steel sphere between 2 and 3 cm, with a resulting mass of 0.011 - 0.113 kg [18], [2]. We set the relative velocity to 11 km/s as this was the median velocity of impacts observed by LeoLabs [21]. NASA estimated the mass of the primary object above 100kg [3]. The parameters for the H-IIA fragmentation event are summarized in Table 3.

Table 3: NASA SBM Parameters: H-IIA Launch Vehicle

| Model Inputs | Value | Units |
|---|---|---|
| Primary Object Mass | 100 | kg |
| Primary Object Radius | 8.0 | m |
| Secondary Object Mass | 0.011 - 0.113 | kg |
| Secondary Object Radius | 0.02 - 0.03 | m |
| Relative Velocity | 11 | km/s |

#### 4.3.1 A/M Distribution

To compare the A/M distributions through the range of possible masses involved in the collision, we sampled four sets of parameters along the range. Similar to our previous comparisons for COSMOS 1408 and CZ6A, we limit the analysis to fragments with a characteristic length between 10cm and 1m. The results can be seen in Figures 5 and 6
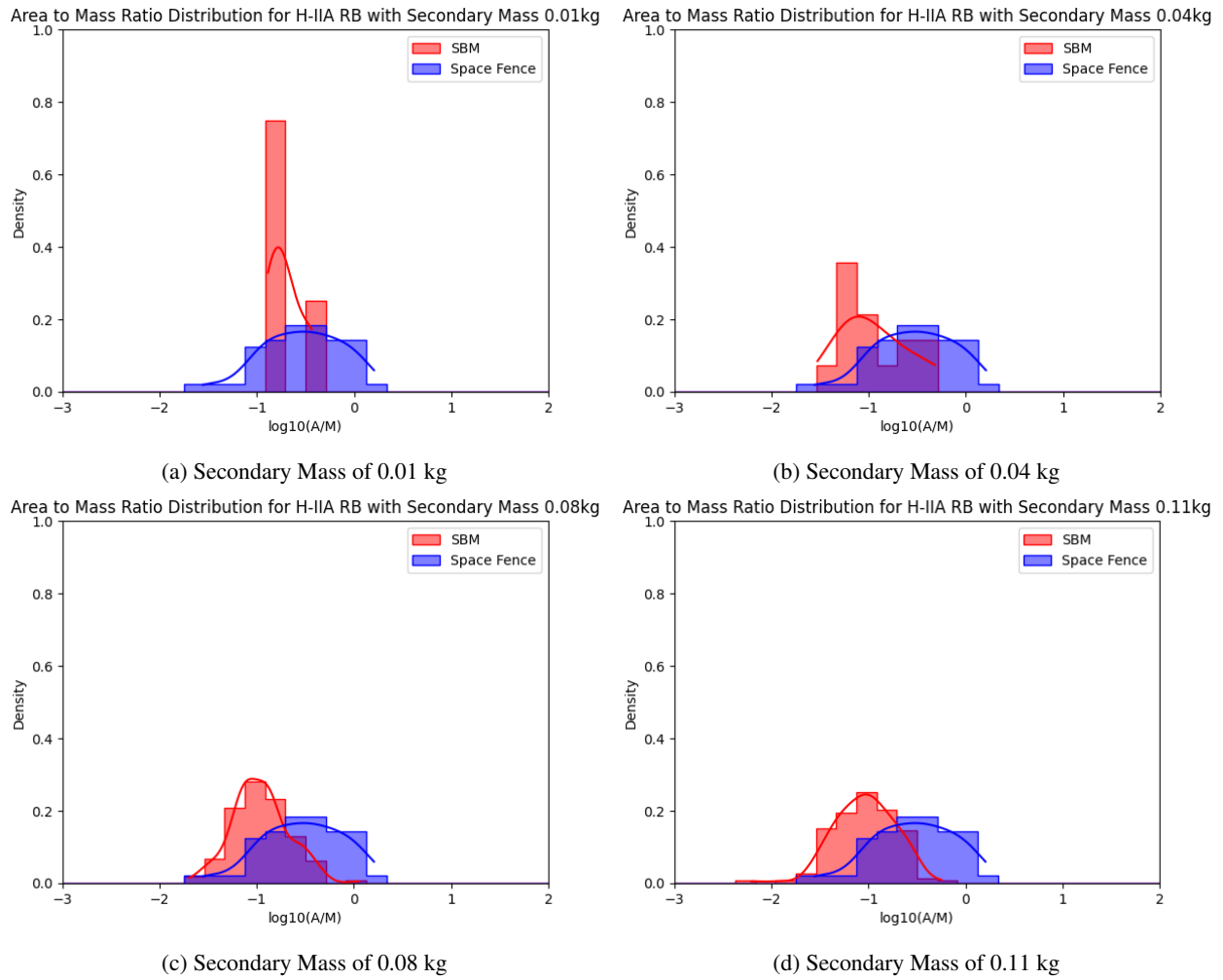
(a) Secondary Mass of 0.01 kg

(b) Secondary Mass of 0.04 kg

(c) Secondary Mass of 0.08 kg

(d) Secondary Mass of 0.11 kg

Fig. 5: $log_{10}(A/M)$ distribution comparison between Space Fence data and the NASA SBM for the HIIA collision with varying secondary masses and relative velocity of 11 km/s.
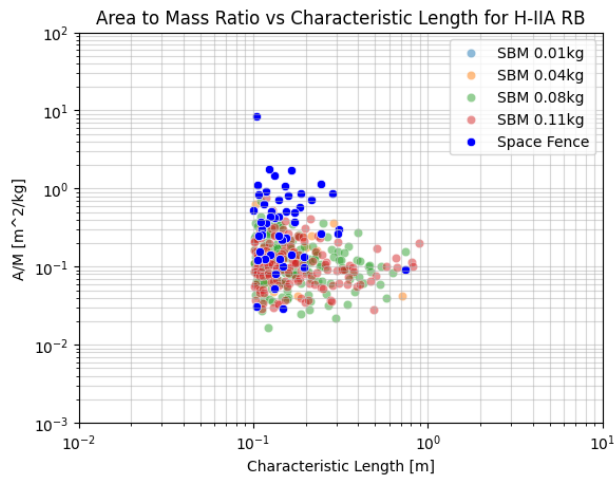


Fig. 6: A/M Vs. Characteristic Length comparison between Space Fence data and the NASA SBM for the HIIA collision with varying secondary masses and relative velocity of 11 km/s.

It's evident from these results, that the SBM does not match well across the range of possible collision scenarios. As there are many unknowns about this event, it's possible that some factor about the collision not considered could shift the distribution of the SBM to better match that of Space Fence. At least under our estimated parameters, however, the SBM estimates a tighter distribution for the A/M around $0.10 \frac{m^2}{kg}$, while the Space Fence data is wider with a median closer to $0.05 \frac{m^2}{kg}$.

### 4.3.2 $\Delta V$ Distribution

When comparing the $\Delta V$ distributions, we used the same sample secondary masses from our estimated mass range shown in Table 3 as we used in the A/M results. The results for our comparison can be seen in Fig. 7.



(a) Secondary Mass of 0.01 kg

(b) Secondary Mass of 0.04 kg

(c) Secondary Mass of 0.08 kg

(d) Secondary Mass of 0.11 kg
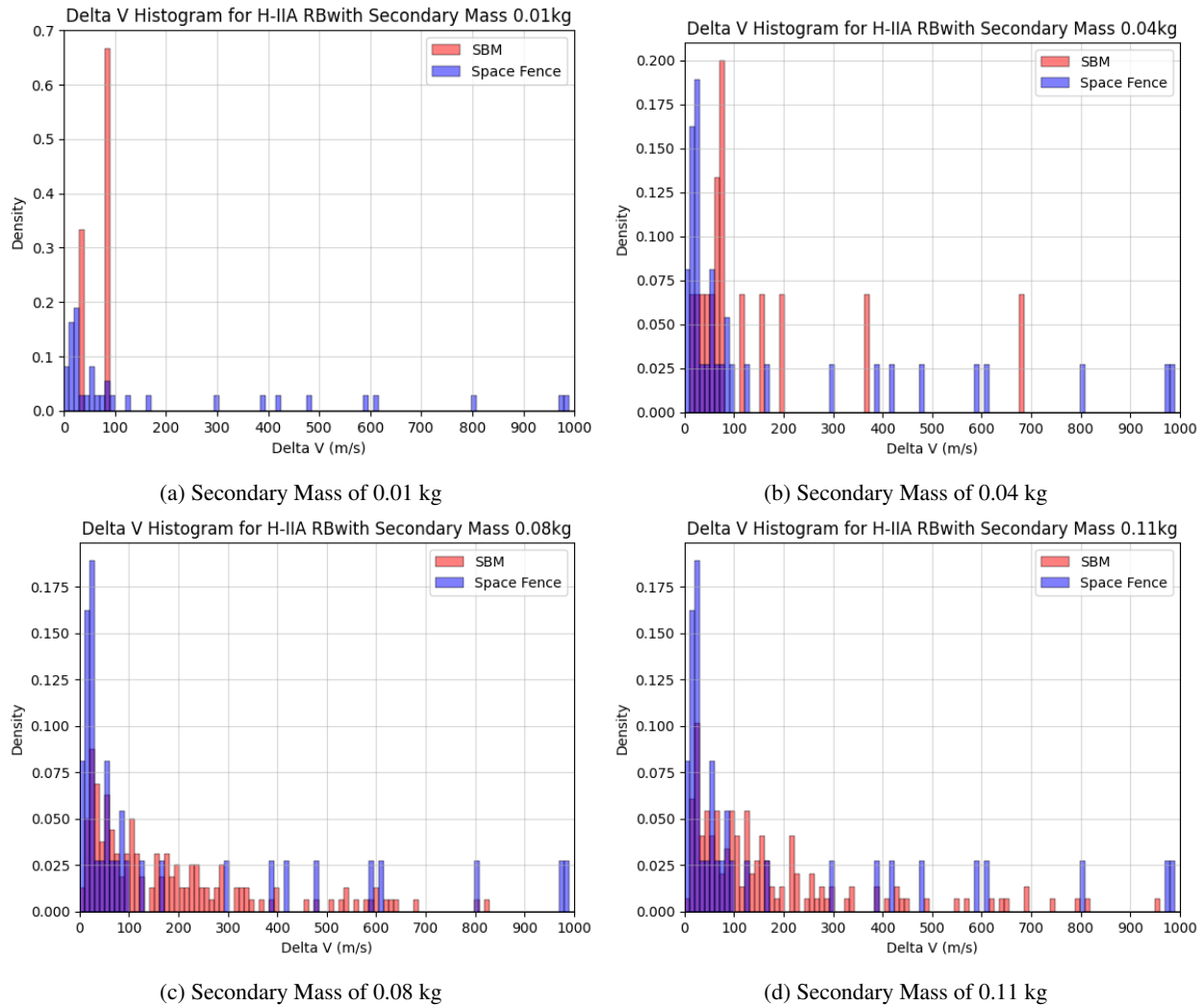
Fig. 7: $\Delta V$ distribution comparison between Space Fence data and the NASA SBM for the HIIA collision with varying secondary masses and relative velocity of 11 km/s.

Similar to what we found with the COSMOS 1408 collision, the SBM generally overestimates the $\Delta V$ of the fragments when compared against the observations made by Space Fence. Notably, the piece-wise nature of the SBM for catastrophic vs. non-catastrophic collisions is made apparent in the transition from the secondary mass of 0.04kg to 0.01kg. However, in neither case is the scenario captured well by the SBM.

## 4.4 COSMOS 2499

The fragmentation of the COSMOS 2499 satellite is assumed to be caused by an explosion due to the presence of multiple energy storage devices [3]. The parameters used in the SBM are summarized in Table 4.

Table 4: NASA SBM Parameters: COSMOS 2499

| Model Inputs | Value | Units |
|---|---|---|
| Primary Object Mass | 50 | kg |
| Primary Object Radius | assumed to be $> 1$ | m |

### 4.4.1 A/M Distribution

The A/M distributions between the SBM and the Space Fence observations were again limited to comparison of objects between 10cm and 1m due to the limitations of the S-band trackability and SBM power law. The results of this comparison can be seen in Fig. 8



(a) A/M Vs. Characteristic Length

(b) $log_{10}(A/M)$ Distribution
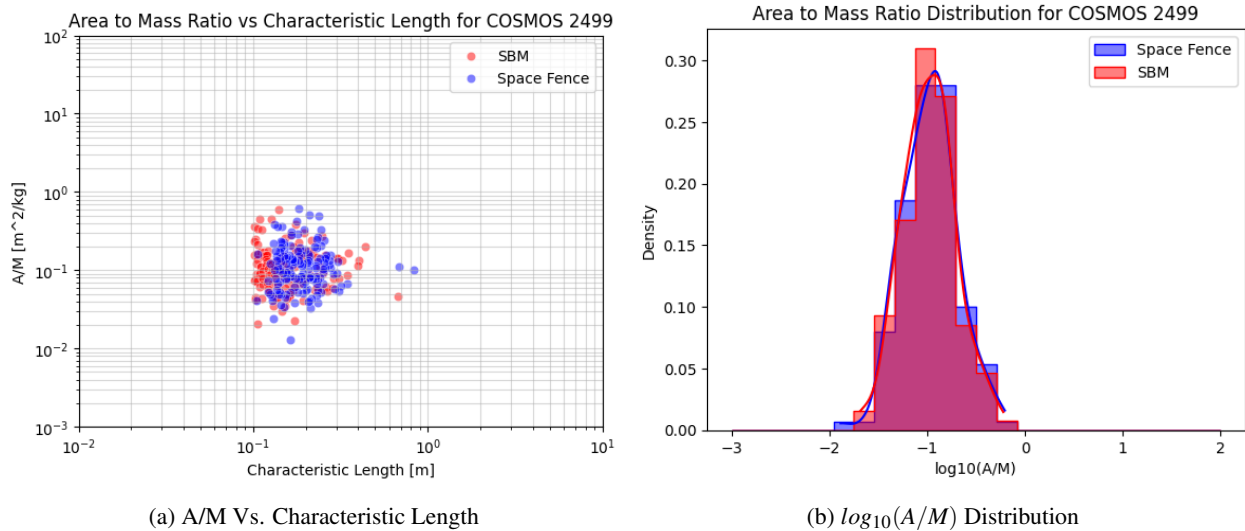
Fig. 8: A/M distribution comparison between Space Fence data and the NASA SBM for the 2499 fragmentation event modeled as an explosion

Similar to what was found for the CZ6A explosion, the A/M distributions between what was estimated by the SBM and observations collected by Space Fence match closely. As the A/M estimations are stochastic for both the Space Fence data and the SBM, some slight variation between runs of the model do produce varying results with less agreement. However, across model runs, both distributions are tightly centered around an A/M of 0.10 $\frac{m^2}{kg}$ and we consider this event well captured by the SBM.

### 4.4.2 $\Delta V$ Distribution

As with the previous events the $\Delta V$ distribution is limited to the 10cm to 1m margins due to the inconsistency of detection below 10cm and objects no longer following the power law in the SBM above 1m. The results of the comparison for the 2499 event modeled as an explosion can be seen in Fig. 9
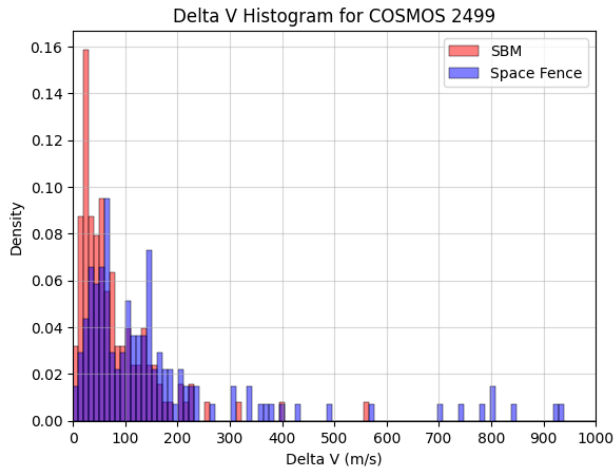
Fig. 9: $\Delta V$ distribution comparison between Space Fence data and the NASA SBM for the 2499 fragmentation event modeled as an explosion

Unlike the previous events, the SBM seems to overestimate the number of objects with a lower $\Delta V$ as compared to the data collected by Space Fence. The CvM bootstrapped p-value for the two distributions is 0.1765, further indicating a lack of correlation. The inconsistent pattern of $\Delta V$ from explosions between CZ6A and this event highlights the challenges in developing a general model for such events as there are many factors that can drastically affect the behavior of fragments generated.

### 4.5 Orbcomm FM36

Similar to COSMOS 2499 the fragmentation of the Orbcomm FM36 satellite is assumed to be an explosion due to the energy storage devices associated with the satellite [3]. The mass of Orbcomm FM36 is known to be 42 kg with a radius of 3.5 m based on the manufacturer's information [29]. The parameters used in our NASA SBM implementation for the Orbcomm FM36 fragmentation event can be seen in Table 5.

Table 5: NASA SBM Parameters: Orbcomm FM36

| Model Inputs | Value | Units |
|---|---|---|
| Primary Object Mass | 42 | kg |
| Primary Object Radius | 3.5 | m |

#### 4.5.1 A/M Distribution

We again limited our comparison of the A/M distributions between the observations made by Space Fence and the SBM between objects with a lower bound characteristic length of 10cm and upper bound of 1m due to the S-Band observation and SBM power-law limitations. The results of our comparison can be seen in Fig. 10

(a) A/M Vs. Characteristic Length

(b) $log_{10}(A/M)$ Distribution
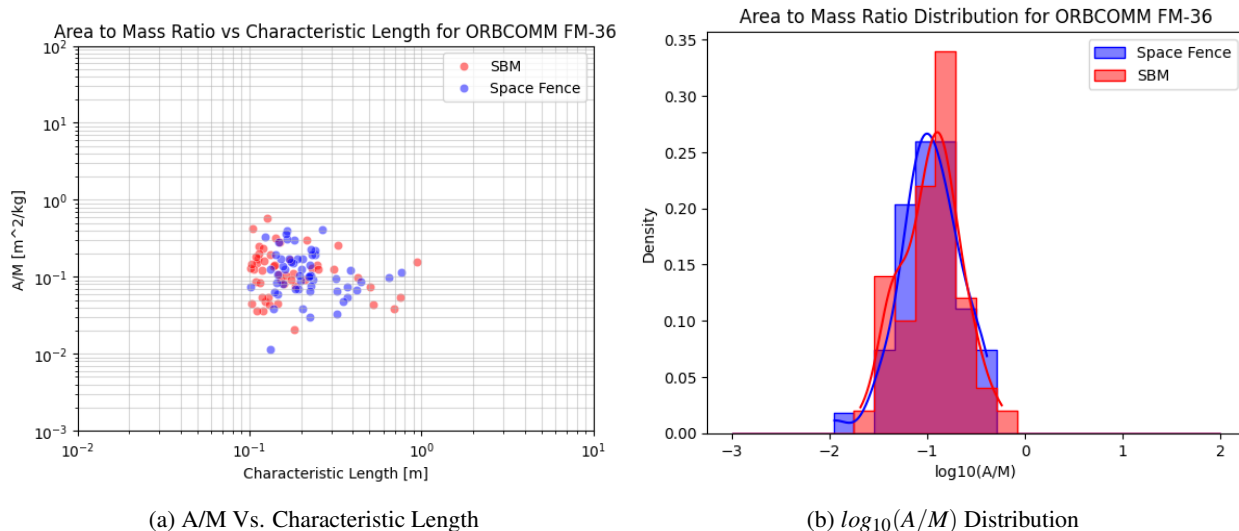
Fig. 10: A/M distribution comparison between Space Fence data and the NASA SBM for the 2499 fragmentation event modeled as an explosion

For this event, we see a close correlation between the estimated distribution by the SBM and distribution of objects collected by Space Fence with both distributions centred around a A/M of 0.10 $\frac{m^2}{kg}$. As with the others, we consider the A/M distribution of the event captured well by the SBM.

### 4.5.2 $\Delta V$ Distribution

Using the same margins described previously, the $\Delta V$ distributions for the Orbcomm FM-36 event estimated by the SBM compared to the observations made by Space Fence can be seen in Fig. 11.
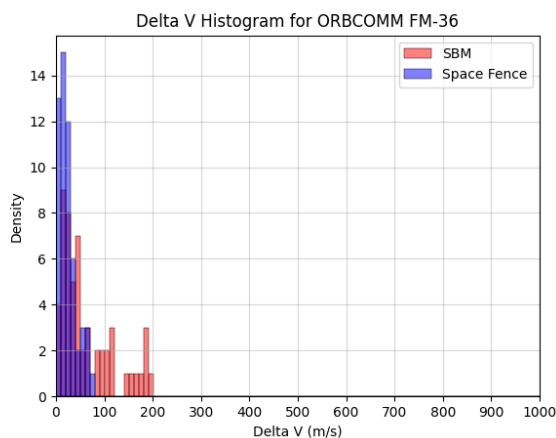


Fig. 11: $\Delta V$ distribution comparison between Space Fence data and the NASA SBM for the Orbcomm Fm-36 fragmentation event modeled as an explosion

The results for this event follow a familiar pattern to those seen in Fig. 2 and 4 for COSMOS 1408 and CZ-6A respectively in that the SBM generally overestimates the $\Delta V$ of the objects generated. Our bootstraped p-value also suggests a lack of correlation between the distributions with a value of 0.0002.

# 5. DISCUSSION

The results of our comparison between the NASA SBM and observations made by Space Fence when comparing the A/M and $\Delta V$ distributions for the five fragmentation events described in 2 demonstrate areas where the SBM is successful in capturing an event and where deficiencies are apparent. Generally, the SBM performs well when estimating the A/M distributions with strong correlations among most of the events examined, with the exception of the HII-A collision event. However, this event lacks the most information due to the many uncertainties surrounding the secondary object involved. This makes it difficult to completely attribute the differences between the model and empirical data to deficiencies in the model. This event highlights the challenges involved in developing a generally applicable model with so few examples and limited observability of the events that do exist. Perhaps the most unfortunate aspect of our limited capacity to observe these events due to our reliance on ground-based sensors is our inability to examine the model in its entirety against on-orbit events. As mentioned in 4, the limits of the S-band radar meant that we were unable to form tracks for many objects detected below 10cm. This prevented us from comparing the empirical results with the A/M distributions for objects with a characteristic length below 8cm as described in Eq. 6. The only viable method for this comparison, and how the model was originally developed for this range, is through ground-based tests, which are even fewer in number than the on-orbit events observed. In addition, we are reliant on the A/M model portion of the SBM for converting the RCS measurements made by Space Fence. This makes it difficult to make a true comparison with the empirical data.

Where we can make a more thorough comparison and do see a more consistent deviation between the estimated distributions made by the SBM and the empirical observations collected by Space Fence is in the $\Delta V$ distributions. We are still limited to comparisons between objects with characteristic lengths between 10cm and 1m, but we are only reliant on the A/M portion of the SBM for estimating the ballistic coefficient of the objects for propagation purposes with SGP4. In all of the events, we saw a lack of correlation between the SBM and empirical data. The SBM generally overestimates the $\Delta V$ of the fragments generated by the event with the only exception being the COSMOS 2499 event, which saw the opposite. This outlier again demonstrates the difficulty in developing a model consistent with all events, as there are many factors involved that can drastically affect the behavior of the fragments.

The NASA SBM has become the standard for many reasons, it's lightweight, has shown capability in capturing aspects of some events accurately and has been useful in contributing to future space environment forecasts. However, there are some still some deficiencies as we've highlighted here and others have discovered with modern ground-based tests [24] and comparison to numerical simulations [32].

# 6. CONCLUSION AND FUTUREWORK

In this paper, we compared the A/M and $\Delta V$ distributions generated by the NASA SBM to the observations collected by Space Fence for five fragmentation events: COSMOS 1408, Chang Zheng 6A, H-IIA Rocket Body, COSMOS 2499 and Orbcomm FM-36. We found that the model captures the A/M distributions of these events well, but has significant discrepancies between the estimated $\Delta V$ distributions and the empirical data. The inconsistencies between the estimations and empirical data, and between the events themselves, highlights the many challenges involved when developing a generally applicable and lightweight break-up model.

No model will ever be able to capture all specifics and complexities involved with every event, at least not without significant computational demands and perfect knowledge of the parameters surrounding each event. We are thus reliant on imperfect models such as the SBM to assist us in making determinations and estimations with consideration of their deficiencies. That does not mean we shouldn't continue to improve our modeling capabilities as new techniques for analysis and data becomes available.

We propose that there is an opportunity with the data we have collected here, combined with simulated data generated by high-fidelity physics-based models to train a machine learning model which can more effectively capture the complexity of the events while maintaining a general applicability and lightweight form factor. In future work, we will explore this methodology and compare the results against the SBM and other break-up models, as well against empirically collected data from Space Fence.

# 7. ACKNOWLEDGEMENT

# 8. REFERENCES

[1] CelesTrak: Astrodynamics Software by David Vallado.

[2] Encyclopedia of Physical Science and Technology. ISBN: 9780122274107.

[3] Orbital Debris Quarterly News 28-3.

[4] Orbital Debris Quaterly News 26-3.

[5] Space-Track.org.

[6] U.S. Strengthening Space Domain Awareness.

[7] 18th & 19th SDS. SFS Handbook for Satellite Operators, April 2023.

[8] T. W. Anderson. On the Distribution of the Two-Sample Cramér-von Mises Criterion. *The Annals of Mathematical Statistics*, 33(3):1148–1159, 1962. Publisher: Institute of Mathematical Statistics.

[9] ATK. ATK Space Propulsion Products Catalog, 2008.

[10] Vitali Braun, André Horstmann, Stijn Lemmens, Carsten Wiedemann, and Lorenz Böttcher. Recent developments in space debris environment modelling, verification and validation with MASTER. 2021.

[11] Andrea D'Ambrosio, Miles Lifson, and Richard Linares. The Capacity of Low Earth Orbit Computed using Source-sink Modeling, June 2022. arXiv:2206.05345 [physics].

[12] Alessandro Francesconi, Cinzia Giacomuzzo, Lorenzo Olivieri, Giulia Sarego, Matteo Duzzi, Francesco Feltrin, Andrea Valmorbida, Karl Dietrich Bunte, Meenakshi Deshmukh, Esfandiar Farahvashi, Jewel Pervez, Matthias Zaake, Tiziana Cardone, and Don De Wilde. CST: A new semi-empirical tool for simulating spacecraft collisions in orbit. *Acta Astronautica*, 160:195–205, July 2019.

[13] S. Ghio and M. Martorella. Size estimation of space debris models from their RCS measured in anechoic chamber. In *2020 17th European Radar Conference (EuRAD)*, pages 421–424, January 2021.

[14] Daniel Jang, Davide Gusmini, Peng Mun Siew, Andrea D'Ambrosio, Simone Servadio, Pablo Machuca, and Richard Linares. *Monte Carlo Methods to Model the Evolution of the Low Earth Orbit Population*. January 2023.

[15] N.L. Johnson, Paula Krisko, J.-C Liou, and Phillip Anz-Meador. NASA's new breakup model of evolve 4.0. *Advances in Space Research*, 28:1377–1384, December 2001.

[16] Andrew Jones. Chinese rocket body breaks up in orbit after successful satellite launch, 2022.

[17] Heiner Klinkard. *Space Debris*. Springer Praxis Books. Springer Berlin Heidelberg, 2006.

[18] M. Kluziak. Aluminum Weight Calculator, 2024.

[19] P. H. Krisko. Proper Implementation of the 1998 NASA Breakup Model.

[20] P. H. Krisko, S. Flegel, M. J. Matney, D. R. Jarkey, and V. Braun. ORDEM 3.0 and MASTER-2009 modeled debris population comparison. *Acta Astronautica*, 113:204–211, August 2015.

[21] LeoLabs. Analysis of the Cosmos 1408 Breakup, November 2021.

[22] Pascal Matura, Georg Heilig, Martin Lueck, and Martin Sauer. Simulation and Experiments of Hypervelocity Impact in Containers with Fluid and Granular Fillings. *Procedia Engineering*, 103:365–372, January 2015.

[23] Darren McKnight, Robert Maher, and Larry Nagl. Refined algorithms for structural breakup due to hypervelocity impact. *International Journal of Impact Engineering*, 17(4-6):547–558, January 1995.

[24] James Murray and Heather Cowardin. Analysis of the DebriSat Fragments and Comparison to the NASA Standard Satellite Breakup Model. page 10, 2019.

[25] ODPO. Orbital Debris Quarterly News 26-3. Technical report.

[26] ESA Space Debris Office. ESA'S ANNUAL SPACE ENVIRONMENT REPORT. Technical report, July 2024.

[27] D. et al Oltrogge. RUSSIAN ASAT DEBRIS CLOUD EVOLUTION AND RISK, 2022. Publisher: COMSPOC.

[28] Daniel L. Oltrogge and David A. Vallado. Debris Risk Evolution And Dispersal (DREAD) for post-fragmentation modeling. American Society of Mechanical Engineers Digital Collection, June 2020.

[29] Orbital. Orbcomm FM1 - FM43, 2014.

[30] Passant Rabie. Chinese Rocket Stage Now a Cloud of Orbital Debris After Disintegrating in Space, 2022. Publisher: Gizmodo.

[31] Raytheon. Exoatmospheric Kill Vehicle/Ground-based Midcourse Defense System, 2002.

[32] Martin Schimmerohn. Numerical investigation on the standard catastrophic breakup criteria. September 2020.

[33] Jonas Schuhmacher. *Efficient Implementation and Evaluation of the NASA Breakup Model in modern C++*. Bachelor's Thesis, 2021.

[34] Tory Smith, Jacqueline Smith, Zachary Folcik, and Richard Linares. Examining the accuracy of the NASA Standard Break-up Model using Space Fence data.

[35] H. K. Springer, W. O. Miller, J. L. Levatin, A. J. Pertica, and S. S. Olivier. Satellite Collision Modeling with Physics-Based Hydrocodes: Debris Generation Predictions of the Iridium-Cosmos Collision Event and Other Impact Events. Technical Report LLNL-CONF-454151, Lawrence Livermore National Lab. (LLNL), Livermore, CA (United States), September 2010.

[36] David A. Vallado. *Fundamentals of astrodynamics and applications*. Space technology library. Microcosm Press, Torrance, CA, fifth edition edition, 2022.

[37] E. Watson, H.-G. Maas, F. Schäfer, and S. Hiermaier. TRAJECTORY BASED 3D FRAGMENT TRACKING IN HYPERVELOCITY IMPACT EXPERIMENTS. *The International Archives of the Photogrammetry, Remote Sensing and Spatial Information Sciences*, XLII-2:1175–1181, May 2018. Conference Name: ISPRS TC II Mid-term Symposium <q>Towards Photogrammetry 2020</q> (Volume XLII-2) - 4&ndash;7 June 2018, Riva del Garda, Italy Publisher: Copernicus GmbH.

[38] Y.-I. Xu, C. Stokely, M. Matney, and E. Stansbery. A Statistical Size Estimation Model for Haystack a... In *56th International Astronautical Congress of the International Astronautical Federation, the International Academy of Astronautics, and the International Institute of Space Law*, Fukuoka, Japan, October 2005. American Institute of Aeronautics and Astronautics.